UDC 550.89

THE ADIABATIC GRADIENT IN THE TRANSITIONAL MANTLE ZONE: DIVARIANT TRANSFORMATIONS*

L. M. Truskinovskiy, O. L. Kuskov and N. I. Khitarov (deceased)

Vernadskiy Institute of Geochemistry and Analytical Chemistry, Academy of Sciences of the USSR, Moscow

The paper deals with simulating the structure of the divariant heterophase region in a convecting mantle and with simulating the adiabatic temperature distribution with allowance for the heat sources due to phase transformations. Differential equations are derived for the pressure dependence of the phase compositions, which are generalizations of van der Waals relations. These are used in an expression for dT/dP along the adiabat. As an example, the transformation of olivine-spinel into a continuous series of ideal forsterite-fayalite solid solutions is considered, which simulates the seismic boundary at a depth of ~400 km.

Convective models for the Earth indicate that the temperature distribution at depth should be close to adiabatic (isentropic)** everywhere apart from fairly narrow thermal boundary layers separating independently convecting regions [1, 2]. Determining the temperature at depth is closely related to the chemical and phase compositions of mantle shells, where the construction of the adiabat should be based on knowledge of the chemical structures in the corresponding regions. Particular interest attaches to the adiabat structure in heterophase zones, where allowance is made for the compositional variations in coexisting phases. Phase transformations involving heat release or absorption occur in such zones where they are penetrated by convective flows, and this affects the adiabatic temperature gradient.

We have considered the adiabat structure in the region of a heterophase boundary corresponding to a univariant transformation in constant-composition phases in [4], where we also examined the applicability of the adiabatic model in considering flows through zones having internal heat sources. Here we extend the results obtained in [4] to divariant transformation in multi-component solid solutions. As in [4], we calculated the equilibrium isentrope in P–T coordinates, which is readily transformed to the geotherm, since the depth dependence of the pressure is known. This division of the mechanical treatment from the thermal one enables us to examine the thermal aspect in detail by chemical-thermodynamic methods.

Ferromagnesian solid solutions in the MgO-FeO-SiO_2 system are important to the geochemical structure of the mantle, so we will consider divariant transformations in an n-component system by reference to the phase transition of olivine-spinel into a continuous series of forsterite-fayalite solid solutions. The corresponding three-dimensional state diagram in P, T, and x coordinates is constructed on the assumption that the *Fo*–*Fa* solid solutions are ideal [5]. The diagram has been based on thermodynamic information on the pure phases obtained by the potential method [6].

We know of only one paper [7] dealing with the adiabat in a solid-state divariant region for a binary system, although this did not obtain final results for the general case, since special assumptions were made about the

*Translated from Geokhimiya, No. 5, pp. 579-593, 1985.

**We do not distinguish the adiabat and the isentrope, on the assumption that dissipative processes may be neglected [3].

ISSN0016-7029/85/0008-0047$7.50/0

behavior of the thermodynamic functions, and in particular mixing effects were ignored. Adiabat construction has been considered also [8] in relation to mantle melting in the presence of volatiles. Here we will perform an independent study of an n-component system that provides explicit equations for the derivative $dT/dP_{(A)}$ along the adiabat and calculate the corresponding values for the olivine-spinel transformation. Previously, conflicting assertions have been made on the adiabatic gradient in the divariant region where olivine and spinel coexist (see, for example, [7]).

Brief information has been given on some of the present results in [9].

CASE OF AN n-COMPONENT SYSTEM

Consider the heterogeneous equilibrium between r phases in an n-component system. Let P and T be the pressure and temperature; by x_i^α we denote the molar concentration of the component with index i ($i = 1, \ldots n$) in the phase with index α

$$(\alpha = 1, \ldots r)\left(\sum_{i=1}^{n} x_i^\alpha = 1\right).$$

According to the conditions for phase equilibrium,

$$\mu_i^1(P, T, x_j^1) = \cdots = \mu_i^r(P, T, x_j^r), \tag{1}$$

where μ_i^α is the chemical potential of component i in phase α [10]. We denote by ξ_α the molar proportion of phase α in the closed system,*

$$\sum_{\alpha=1}^{r} \xi_\alpha = 1.$$

We specify the overall chemical composition

$$\overset{0}{x}_i, \sum_{i=1}^{n} \overset{0}{x}_i = 1;$$

where the following equations apply

$$\sum_{\alpha=1}^{r} x_i^\alpha \xi_\alpha = \overset{0}{x}_i, \quad i = 1, \ldots n. \tag{2}$$

The adiabatic (isentropic) condition can then be written as

$$S(\xi_\beta, x_j^\beta, PT) \equiv \sum_{\alpha=1}^{r} \xi_\alpha S^\alpha(P, T, x_i^\beta) = S_0, \tag{3}$$

where S_0 is the specified molar entropy of the heterogeneous mechanical mixture, while S^α are the molar entropies of the individual phases. The required $T_A(P)$ relationships are now determined from a system of $rn + 1$ equations (1-3), which contain rn independent variables. The adiabat parameters are the composition $\overset{0}{x}_i$ and the entropy S_0. Clearly, instead of S_0 we could specify the temperature for a certain pressure $T_A(P_0)$.

We now calculate the adiabatic gradient $(dT/dP)_A$ in the divariant region, i.e., subject to the condition that the number of phases equals the number of

*Closure means that in this case one can neglect diffusion.

components, $r = n$. We write equations (1-3) in differential form [11]

$$S^\alpha \, dT - V^\alpha \, dP + \sum_{i=1}^{n} x_i^\alpha \, d\mu^i = 0, \tag{4}$$

$$\sum_{\alpha=1}^{n} (x_i^\alpha \, d\xi_\alpha + \xi_\alpha \, dx_i^\alpha) = 0, \tag{5}$$

$$\sum_{\alpha=1}^{n} \left(\xi_\alpha \frac{\partial S^\alpha}{\partial P} dP + \xi_\alpha \frac{\partial S^\alpha}{\partial T} dT + \xi_\alpha \sum_{i=1}^{n} \frac{\partial S^\alpha}{\partial x_i^\alpha} dx_i^\alpha + S^\alpha \, d\xi_\alpha \right) = 0, \tag{6}$$

where μ_i is the chemical potential of component i, which is the same in all phases, while S^α and V^α are the molar entropy and volume of phase α. Then equations (4) are clearly Gibbs-Duhem equations [10]. We take the matrix $\boldsymbol{X} = \|x_i^\alpha\|$ as nondegenerate (det $\boldsymbol{X} \neq 0$), to get from (4) via Kramer's formula [12] that

$$d\mu^i = \frac{D_V^i}{D_X} dP - \frac{D_S^i}{D_X} dT \equiv \frac{\sum_{\alpha=1}^{n} y_\alpha^i V^\alpha}{D_X} dP - \frac{\sum_{\alpha=1}^{n} y_\alpha^i S^\alpha}{D_X} dT, \tag{7}$$

where $D_X = \det \boldsymbol{X}$ and $D_{V,S}^i$ are the determinants of matrix $\boldsymbol{X}_{V,S}$ derived from $\boldsymbol{X}$ by replacing column i correspondingly by $\{V^\alpha\}$ or $\{S^\alpha\}$, while $y_i{}^\alpha$ is the algebraic complement of element $x_i{}^\alpha$ in matrix $\boldsymbol{X}$ [12]. On the other hand, the differential $d\mu_i{}^\alpha$ can be represented for each of the phases in the form

$$d\mu_i^\alpha = -\bar{S}_i^\alpha \, dT + \bar{V}_i^\alpha \, dP + \sum_{j=1}^{n-1} \frac{\partial \mu_i^\alpha}{\partial x_j^\alpha} dx_j^\alpha, \tag{8}$$

where $\bar{S}_i{}^\alpha = \partial S^\alpha / \partial x_i{}^\alpha$, $\bar{V}_i{}^\alpha = \partial V^\alpha / \partial x_i{}^\alpha$ are the partial molar entropy and volume of component i in phase α. We combine (7) and (8) to get

$$\sum_{j=1}^{n-1} \frac{\partial \mu_i^\alpha}{\partial x_j^\alpha} dx_j^\alpha = \left[\frac{\partial S^\alpha}{\partial x_i^\alpha} - \frac{D_S^i}{D_X} \right] dT - \left[\frac{\partial V^\alpha}{\partial x_i^\alpha} - \frac{D_V^i}{D_X} \right] dP. \tag{9}$$

We take the matrix $\boldsymbol{M} = \|\partial \mu_i{}^\alpha / \partial x_j{}^\alpha\|$ ($i = 1, \ldots n-1$, $j = 1, \ldots n-1$) as nondegenerate, which gives us a generalization of the van der Waals equations [13] obtained for divariant equilibria in binary systems:

$$\left. \frac{\partial x_j^\alpha}{\partial T} \right|_P = \frac{\sum_{i=1}^{n-1} M_{ji}^\alpha \left(\frac{\partial S^\alpha}{\partial x_i^\alpha} - \frac{D_S^i}{D_X} \right)}{D_M^\alpha}, \tag{10}$$

$$\left. \frac{\partial x_j^\alpha}{\partial P} \right|_T = -\frac{\sum_{i=1}^{n-1} M_{ji}^\alpha \left(\frac{\partial V^\alpha}{\partial x_i^\alpha} - \frac{D_V^i}{D_X} \right)}{D_M^\alpha}, \tag{11}$$

where M_{ji}^α is the algebraic complement [12] of the element $\partial \mu_i{}^\alpha / \partial x_j{}^\alpha$ in matrix $\boldsymbol{M}$. Equations (10) and (11) enable us to determine the pressure and temperature dependence of the equilibrium concentrations in the divariant n-phase region.

From the derivatives of (10) and (11) and from (5) we can calculate the P and T dependence of the phase composition. We use the nondegeneracy of $\|x_i{}^\alpha\|$ to get

$$d\xi_\alpha = \left[\sum_{i=1}^{n} \sum_{k=1}^{n-1} y_\alpha^i M_{ik}^\alpha \left(\frac{\partial V^\alpha}{\partial x_k^\alpha} - \frac{D_V^k}{D_X} \right) dP - \sum_{i=1}^{n} \sum_{k=1}^{n-1} y_\alpha^i M_{ik}^\alpha \left(\frac{\partial S^\alpha}{\partial x_k^\alpha} - \frac{D_S^k}{D_X} \right) dT \right] \frac{\xi_\alpha}{D_X D_M^\alpha}. \tag{12}$$

The temperature dependence of the pressure can now be determined by means of the adiabatic condition (6). We express dx_i^α and $d\xi_\alpha$ as functions of dP and dT to get

$$\sum_{\alpha=1}^{n} \xi_\alpha \left[\frac{\partial S^\alpha}{\partial P} - \sum_{i=1}^{n} \sum_{k=1}^{n-1} \frac{M_{ki}^\alpha}{D_M^\alpha} \left[\frac{\partial V^\alpha}{\partial x_k^\alpha} - \frac{D_V^k}{D_X} \right] \left[\frac{\partial S^\alpha}{\partial x_i^\alpha} - \frac{D_S^i}{D_X} \right] \right] dP + \\ + \sum_{\alpha=1}^{n} \xi_\alpha \left[\frac{\partial S^\alpha}{\partial T} + \sum_{i=1}^{n} \sum_{k=1}^{n-1} \frac{M_{ki}^\alpha}{D_M^\alpha} \left[\frac{\partial S^\alpha}{\partial x_k^\alpha} - \frac{D_S^k}{D_X} \right] \left[\frac{\partial S^\alpha}{\partial x_i^\alpha} - \frac{D_S^i}{D_X} \right] \right] dT = 0. \tag{13}$$

The desired expression for the adiabatic gradient $(dT/dP)_A$ follows directly from (13).

In order to explain the general equations, let us consider a detailed example of a divariant two-phase equilibrium in a binary system. For convenience, the analysis of this particular case is performed independently, with equations analogous to (1-13) derived afresh each time.

TWO-PHASE EQUILIBRIUM IN A BINARY SYSTEM

Let us consider a two-component two-phase system. We denote the components by 1 (for example, Fe_2SiO_4) and 2 (Mg_2SiO_4). The assignment to a phase is described by means of the indices α and γ. Let $\overset{0}{x}$ be the molar concentration of component 1 and ξ the degree of transformation (molar proportion of phase α). We denote by x_α the molar concentration of component 1 in phase α and by x_γ the molar concentration of component 1 in phase γ. Then clearly

$$\xi = (\overset{0}{x} - x_\gamma)/(x_\alpha - x_\gamma). \tag{14}$$

It is readily seen that (14) is an analog of (2). The entropy expression is

$$S = [\xi S_\alpha(P, T, x_\alpha) + (1-\xi) S_\gamma(P, T, x_\gamma)], \tag{15}$$

where $S_{\alpha,\gamma}$ are the molar entropies of the phases. The conditions for chemical equilibrium in the two-phase system are represented by the following (see (1)):

$$\mu_\alpha^1(P, T, x_\alpha) = \mu_\gamma^1(P, T, x_\gamma); \quad \mu_\alpha^2(P, T, x_\alpha) = \mu_\gamma^2(P, T, x_\gamma), \tag{16}$$

where $\mu_{\alpha,\gamma}^{1,2}$ are the chemical potentials of components 1 and 2 in phases α and γ. Away from the critical points, equations (16) can be solved for x_α and x_γ:

$$x_\alpha = x_\alpha(P, T), \; x_\gamma = x_\gamma(P, T). \tag{17}$$

We write out the adiabatic (isentropic) condition in differential form:

$$\left[\frac{\partial S_\gamma}{\partial P} - \xi \Delta \left(\frac{\partial S}{\partial P} \right) \right] dP + \left[\frac{\partial S_\gamma}{\partial T} - \xi \Delta \left(\frac{\partial S}{\partial T} \right) \right] dT - \Delta S \, d\xi + \\ + \xi \frac{\partial S_\alpha}{\partial x_\alpha} dx_\alpha + (1 - \xi) \frac{\partial S_\gamma}{\partial x_\gamma} dx_\gamma = 0, \tag{18}$$

where $\Delta f = f_\gamma - f_\alpha$. The differentials dx_α and dx_γ can be expressed in terms of dP and dT by means of (17); as a result, we get van der Waals equations [13] (see [10, 11]):

$$\left. \frac{\partial x_{\alpha,\gamma}}{\partial P} \right|_T = \left(\frac{\partial V}{\Delta x} - \frac{\partial V_{\alpha,\gamma}}{\partial x_{\alpha,\gamma}} \right) \Big/ \frac{\partial^2 G_{\alpha,\gamma}}{\partial x_{\alpha,\gamma}^2}, \\ \left. \frac{\partial x_{\alpha,\gamma}}{\partial T} \right|_P = - \left(\frac{\Delta S}{\Delta x} - \frac{\partial S_{\alpha,\gamma}}{\partial x_{\alpha,\gamma}} \right) \Big/ \frac{\partial^2 G_{\alpha\gamma}}{\partial x_{\alpha,\gamma}^2}, \tag{19}$$

with all quantities in (19) calculated at the equilibrium surface of (17). The molar Gibbs energies of the phases are put as

$$G_{\alpha,\gamma} = x_{\alpha,\gamma} \mu_{\alpha,\gamma}^1 + (1 - x_{\alpha,\gamma}) \mu_{\alpha,\gamma}^2. \tag{20}$$

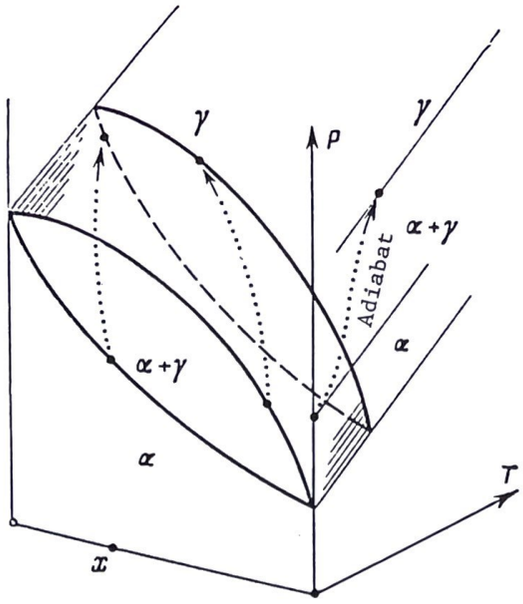

Fig. 1. Schematic representation of the adiabat in P-T-x space for divariant transformation in a binary system, where α and γ are coexisting phases and $\overset{0}{x}$ is a specified bulk concentration.

Equation (14) enables us to express $d\xi$ in terms of dx_α and dx_γ:

$$d\xi = \frac{\overset{0}{x} - x_\alpha}{(\Delta x)^2} dx_\gamma - \frac{\overset{0}{x} - x_\gamma}{(\Delta x)^2} dx_\alpha. \tag{21}$$

We combine (18, 19, 21) to get the equilibrium equation for the two-phase adiabat:

$$dT/dP = -A/B,$$

$$A = \left[\frac{\partial S_\gamma}{\partial P} - \frac{\overset{0}{x} - x_\gamma}{x_\alpha - x_\gamma}\Delta\left(\frac{\partial S}{\partial P}\right)\right] + \left(\frac{\partial x_\alpha}{\partial T}\frac{\partial x_\alpha}{\partial P}\right)\left(\frac{\overset{0}{x} - x_\gamma}{x_\alpha - x_\gamma}\right)\frac{\partial^2 G_\alpha}{\partial x_\alpha^2} + \\ + \left(\frac{\partial x_\gamma}{\partial T}\frac{\partial x_\gamma}{\partial P}\right)\left(\frac{\overset{0}{x} - x_\alpha}{x_\gamma - x_\alpha}\right)\frac{\partial^2 G_\gamma}{\partial x_\gamma^2},$$

$$B = \left[\frac{\partial S_\gamma}{\partial T} - \frac{\overset{0}{x} - x_\gamma}{x_\alpha - x_\gamma}\Delta\left(\frac{\partial S}{\partial T}\right)\right] + \left(\frac{\partial x_\alpha}{\partial T}\right)^2\left(\frac{\overset{0}{x} - x_\gamma}{x_\alpha - x_\gamma}\right)\frac{\partial^2 G_\alpha}{\partial x_\alpha^2} + \\ + \left(\frac{\partial x_\gamma}{\partial T}\right)^2\left(\frac{\overset{0}{x} - x_\alpha}{x_\gamma - x_\alpha}\right)\frac{\partial^2 G_\gamma}{\partial x_\gamma^2}. \tag{22}$$

It can be shown that (22) is the exact analog of (14). In the same way, we can calculate the derivatives $d\xi/dP$, dx_α/dP, and dx_γ/dP. If we substitute the equilibrium concentrations of (17) into (22), we get an ordinary first-order differential equation, whose solution is $T_A(P)$ describing the adiabat in the heterophase region (Fig. 1).

We give the values for $(dT/dP)_A$ (the adiabat slope) at the instant when phase α appears, i.e., at $\xi = 0$, $\overset{0}{x} = x_\gamma$, $T = T_\gamma$, and at the instant when phase γ disappears, i.e., at $\xi = 1$, $\overset{0}{x} = x_\alpha$, $T = T_\alpha$:

$$\left.\frac{dT}{dP}\right|_{T_{\gamma,\alpha}} = \frac{\alpha_{\gamma,\alpha}V_{\gamma,\alpha} - \frac{\partial x_{\gamma,\alpha}}{\partial P}\left[\frac{\partial S_{\gamma,\alpha}}{\partial x_{\gamma,\alpha}} - \frac{\Delta S}{\Delta x}\right]}{\frac{c_{p_{\gamma,\alpha}}}{T} + \frac{\partial x_{\gamma,\alpha}}{\partial T}\left[\frac{\partial S_{\gamma,\alpha}}{\partial x_{\gamma,\alpha}} - \frac{\Delta S}{\Delta x}\right]} \tag{23}$$

Here we have introduced the symbols $c_{p\alpha,\gamma}$ for the phase specific heats and $\alpha_{\alpha,\gamma}$ the coefficients of thermal expansion, both of which are dependent on composition. Equations (23) show that $T_A(P)$ has kinks at the points $T = T_\gamma$ and $T = T_\alpha$, as in the case of univariant equilibria.

The concentration dependence of the thermodynamic functions is specified explicitly for an ideal solution, for example [5, 10]:

$$\mu^1_{\alpha,\gamma} = \overset{0}{\mu}{}^1_{\alpha,\gamma}(P, T) + nRT \ln x_{\alpha,\gamma},$$

$$\mu^2_{\alpha,\gamma} = \overset{0}{\mu}{}^2_{\alpha,\gamma}(P, T) + nRT \ln (1 - x_{\alpha,\gamma}). \tag{24}$$

The quantities $\overset{0}{\mu}{}^{1,2}_{\alpha,\gamma}$ are the molar Gibbs energies of the pure phases. Parameter n arises because the number of formula units does not agree with the number of positions involved in the mixing [5]. For example, in the case of olivine the solution components are usually taken as the cations. Then the number of mixing positions for the Mg^{2+} and Fe^{2+} is double the number of formula units, so $n = 2$.

The expressions for $x_{\alpha,\gamma}$ are readily found from (24):

$$x_\alpha = (1 - \exp \lambda_2)/(1 - \exp(\lambda_2 - \lambda_1)),$$

$$x_\gamma = (1 - \exp \lambda_2)/(\exp \lambda_1 - \exp \lambda_2), \tag{25}$$

where $\lambda_{1,2} = \Delta\overset{0}{\mu}{}^{1,2}/nRT$, $\Delta\overset{0}{\mu}{}^{1,2} = \overset{0}{\mu}{}_\gamma{}^{1,2} - \overset{0}{\mu}{}_\alpha{}^{1,2}$ [14]. We see from (25) that one can construct the equilibrium curves in this approximation, which is equivalent to obtaining thermodynamic information on the pure-phase equilibrium. The following formula gives the chemical potentials of the pure phases at high pressures:

$$\Delta\overset{0}{\mu}{}^i = \Delta\overset{0}{G}{}^i(T) + \int_0^P \Delta\overset{0}{V}{}^i dP. \tag{26}$$

The quantities $\Delta\overset{0}{G}{}^i(T)$ are determined in standard calorimetric experiments and are tabulated in handbooks. The integrals $\int_0^P V dP$ are insensitive to the choice of equation of state and can now be determined with high accuracy over a wide pressure range up to ultrahigh pressures [15].

We use the compositions of the ideal solutions to rewrite (19) as

$$\frac{\partial x_{\alpha,\gamma}}{\partial P} = [x_{\gamma,\alpha}(\Delta\overset{0}{V}{}^1 - \Delta\overset{0}{V}{}^2) + \Delta\overset{0}{V}{}^2] \Big/ \left(\frac{\partial^2 G_{\alpha,\gamma}}{\partial x^2_{\alpha,\gamma}}\right),$$

$$-T\frac{\partial x_{\alpha,\gamma}}{\partial T} = [x_{\gamma,\alpha}(\Delta\overset{0}{H}{}^1 - \Delta\overset{0}{H}{}^2) + \Delta\overset{0}{H}{}^2] \Big/ \left(\frac{\partial^2 G_{\alpha,\gamma}}{\partial x^2_{\alpha,\gamma}}\right);$$

where we have introduced the symbols $\Delta\overset{0}{H}{}^{1,2} = \Delta\overset{0}{\mu}{}^{1,2} + T\Delta\overset{0}{S}{}^{1,2}$. The expressions for the derivatives $\partial^2 G_{\alpha,\gamma}/\partial x^2{}_{\alpha,\gamma}$ can be written out explicitly for ideal solutions:

$$\frac{\partial^2 G_{\alpha,\gamma}}{\partial x^2_{\alpha,\gamma}} = \frac{nRT}{x_{\alpha,\gamma}(1 - x_{\alpha,\gamma})}.$$

The generality of the above equations makes it complicated to derive estimates. The situation simplifies considerably if we are dealing with dilute solutions. The corresponding asymptotic formulas are given in [9].

OLIVINE-SPINEL TRANSFORMATION

A characteristic example of a two-component two-phase system is forsterite (Mg_2SiO_4)-fayalite (Fe_2SiO_4), in which there is the familiar transformation of

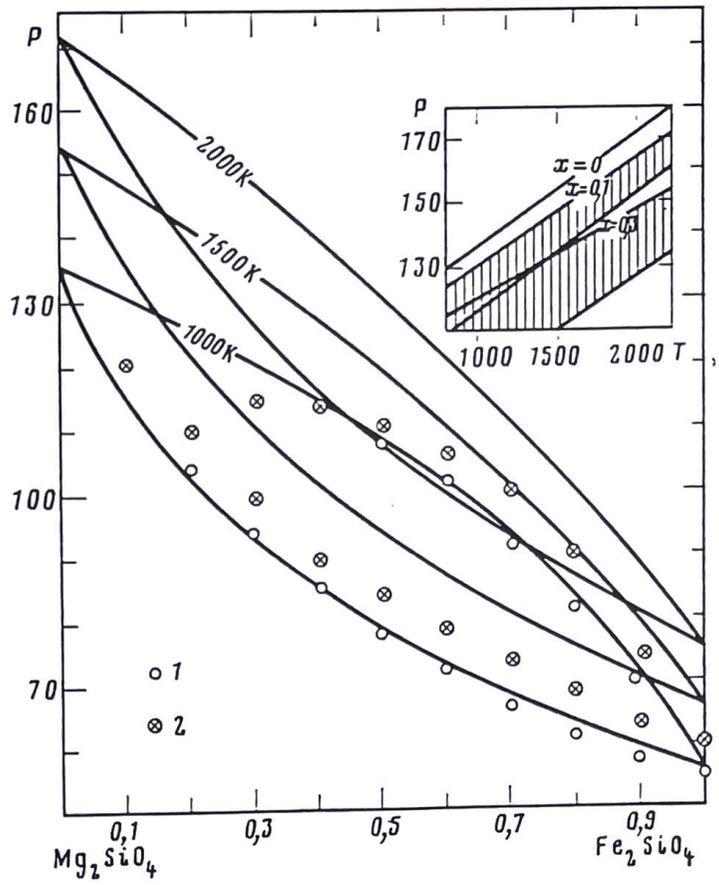

Fig. 2. Isothermal sections of the phase diagram for the olivine-spinel transformation in a continuous series of Mg_2SiO_4-Fe_2SiO_4 solid solutions (neglecting β phase). The lines are by calculation from the ideal-solution model and the points are from experiment (change in pressure calibration scale by ~10 kbar): 1) Akimoto and Fujisawa (800°C), Ringwood and Major (1000°C) [17, 18].

the α phase (olivine) to the denser γ phase (spinel structure). For olivine rich in magnesium, the transformation occurs via an intermediate modified spinel structure (β phase), whose presence can be ignored in view of the model character of the approach. This system deserves particular attention, since the P and T parameters of these transformations are correlated with seismic inhomogeneities in the transitional mantle zone at a depth of ~400 km [1, 2, 4].

To construct the phase diagram for a binary system with ideal mixing, we need thermodynamic information on the pure phases; in this case, these are α-Mg_2SiO_4, α-Fe_2SiO_4, γ-Mg_2SiO_4, and γ-Fe_2SiO_4. All the necessary data can be obtained by the potential method [6, 16]. The molar entropies and volumes of the pure phases are given in Tables 1 and 2 along with the values of $\int_0^P V dP$ and the standard functions ΔG.

Figure 2 (see also Table 3) shows isothermal sections of the equilibrium diagram for the $(Mg_xFe_{(1-x)})_2SiO_4$ system derived from (25), as well as the experimental points of [17].

The diagram is close to the experimental one in the ferroan region if we exclude the pressure shift of ~10 kbar. On the basis of recent determinations of P and T for the phase transitions in pure fayalite and forsterite [18], this systematic deviation is ascribed to erroneous pressure-scale calibration in the early experiments. The agreement is worse in the magnesian region, mainly because of the intermediate phase (β spinel). The discrepancies between the experimental and theoretical diagrams increase somewhat with temperature: for example, the experimental cigar-shaped figure is wider than the theoretical one at $T > 1000$ K, which may be due either to inadequate experimental resolution or to error in the thermal component of the equation of state, which

Table 1

Thermodynamic Parameters of the Pure Phases

P, kbar	α-Fe_2SiO_4			α-Mg_2SiO_4			γ-Fe_2SiO_4			γ-Mg_2SiO_4		
	1000*	1500	2000	1000	1500	2000	1000	1500	2000	1000	1500	2000
					Molar entropies, cal/mol·K							
60	82,8	100,4	113,4	66,5	84,0	96,8	76,1	93,5	106,3	62,6	79,9	92,6
80	82,2	99,8	112,7	65,8	83,2	96,0	75,6	93,0	105,7	62,2	79,4	92,1
100	81,6	99,1	112,0	65,0	82,0	95,3	75,1	92,4	105,2	61,7	78,9	91,5
120	81,0	98,5	111,3	64,6	81,9	94,6	94,6	91,9	104,6	61,2	78,4	91,0
140	80,4	97,9	110,7	64,0	81,3	93,9	74,1	91,4	104,1	60,8	77,9	90,5
160	79,9	97,3	110,3	63,5	80,7	93,4	73,7	91,0	103,8	60,4	77,5	90,0
					Molar volumes, cm^3/mol							
60	45,4	46,2	47,0	42,9	43,7	44,5	41,5	42,1	42,7	39,2	39,8	40,4
80	44,9	45,6	46,4	42,3	43,0	43,8	41,1	41,7	42,3	38,9	39,4	40,0
100	44,4	45,0	45,7	41,8	42,5	43,2	40,7	41,3	41,8	38,6	39,1	39,6
120	43,9	44,5	45,2	41,3	41,9	42,6	40,4	40,9	41,4	38,2	38,7	39,2
140	43,4	44,0	44,6	40,8	41,4	41,6	40,0	40,5	41,0	37,9	38,4	38,9
160	43,0	43,5	44,1	40,4	41,0	41,1	39,7	40,2	40,7	37,6	38,1	38,5
					Integrals $\int_0^P V dP$, kcal/mol							
60	66,51	67,86	68,90	62,91	64,14	65,46	60,45	61,34	62,29	57,02	57,94	58,81
80	88,06	89,53	91,12	83,29	84,87	86,55	80,21	81,35	82,60	75,75	76,85	78,04
100	109,33	111,12	113,04	103,33	105,31	107,33	99,75	101,17	102,68	94,21	95,53	97,00
120	130,35	132,43	134,71	123,25	125,48	127,82	119,13	120,80	122,56	112,56	114,18	115,83
140	151,14	153,52	156,03	142,83	145,34	148,06	138,33	140,23	142,26	130,71	132,54	134,50
160	171,72	174,33	177,14	162,22	165,03	168,04	157,37	159,50	161,77	148,85	150,87	153,02

*T, K.

Table 2

Standard Calorimetric Functions for Transformations in Pure Phases, kcal/mol

T, K	${}^0\Delta G^{\alpha-\gamma}_{Fe_2SiO_4}$	${}^0\Delta G^{\alpha-\gamma}_{Mg_2SiO_4}$	T, K	${}^0\Delta G^{\alpha-\gamma}_{Fe_2SiO_4}$	${}^0\Delta G^{\alpha-\gamma}_{Mg_2SiO_4}$
1000	5,7	11,8	2000	8,0	15,9
1500	6,9	13,8			

accumulates as the temperature increases. On the other hand, one should consider the disordering in the spinels at high temperatures, which may also tend to deform the equilibrium curves.

These diagrams enable us to estimate the minimum width l_0 of the two-phase region corresponding to the isothermal transformation [1]. Here we have to consider the mixture composition. Most of the recent geochemical estimates enable us to select the molar concentration of the fayalite component in the range $0.1 \leqslant \mathring{x} \leqslant 0.2$. For example, Ringwood's pyrolite model [17] leads to $\mathring{x} \sim 0.11$. Taking $\mathring{x} = 0.1$ (90% Mg_2SiO_4, 10% Fe_2SiO_4), we obtain $\delta P \sim 10$-15 kbar and $l_0 \sim 28$-42 km. If we take $\mathring{x} = 0.2$ (80% Mg_2SiO_4, 20% Fe_2SiO_4) we get $\delta P \sim 17$-23 kbar and $l_0 \sim 47$-64 km. The lower bound corresponds to $T = 2000$ K and the upper to $T = 100$ K.

The phase diagram enables us to calculate the distribution of ξ (degree of transformation) in the divariant region; Fig. 3 illustrates $\xi(P)$. We note a feature of these transformations: in the solution $(Mg_{0.9}Fe_{0.1})SiO_4$, the α-γ transformation (at 1000 K) occurs to 60% near the stability region of spinel in the pressure region of 5 kbar (14 km); the complete width of the divariant zone is ~15 kbar (42 km). A similar situation occurs for the iron-rich solutions, where the transformation is localized near the olivine stability region. For intermediate compositions, the transformation occurs uniformly throughout the coexistence region.

The most important characteristic of the adiabat is its slope in the divariant region in T–P coordinates. Table 4 gives calculations from (22) for the entire range in $\mathring{x}$ from 0.1 to 0.9. The following values were used for the specific heats and thermal-expansion coefficients of the pure phases (the mean values for the P and T of Table 4 [4, 16]):

$$c_p \text{ (cal/mol·K)} = 43.3 \ (\alpha\text{-}Fe_2SiO_4);\ 43.0 \ (\gamma\text{-}Fe_2SiO_4);$$
$$43.0 \ (\alpha\text{-}Mg_2SiO_4);\ 42.6 \ (\gamma\text{-}Mg_2SiO_4)$$
$$\alpha \text{ (K}^{-1}) = 3.2\cdot10^{-5} \ (\alpha\text{-}Fe_2SiO_4);\ 2.6\cdot10^{-5} \ (\gamma\text{-}Fe_2SiO_4);$$
$$2.9\cdot10^{-5} \ (\alpha\text{-}Mg_2SiO_4)\ \ 2.4\cdot10^{-5} \ (\gamma\text{-}Mg_2SiO_4).$$

Table 3

Equilibrium Concentrations of the Fayalite Component in $(Fe_xMg_{1-x})_2SiO_4$ Solution

P, kbar	Olivine			γ-spinel		
	1000*	1500	2000	1000	1500	2000
60	0,892	—	—	0,976	—	—
80	0,478	0,712	0,908	0,823	0,891	0,963
100	0,230	0,418	0,599	0,609	0,702	0,799
120	0,074	0,218	0,364	0,298	0,486	0,611
140	—	0,074	0,193	—	0,217	0,396
160	—	—	0,062	—	—	0,155

*T, K

Table 4

Thermodynamic Parameters in the Divariant Two-Phase Region for the Olivine-Spinel Transformation in a Continuous Series of Forsterite-Fayalite Solid Solutions: Degree of Transformation and Adiabatic Gradient

P, kbar	ξ	$\frac{dT}{dP}$, $\frac{K}{kbar}$
$x^0 = 0,1$, $T = 1000$ K		
117,5	0,96	3,22
120	0,89	3.42
122,5	0,79	3,83
125	0,67	4,63
127,5	0,47	6,23
130	0,12	9,54
$x^0 = 0,1$, $T = 1500$ K		
137,5	0,94	5,46
140	0,82	6,07
142,5	0,66	7,12
145	0,43	8,95
147,5	0,04	12,06
$x^0 = 0,1$, $T = 2000$ K		
155	0,93	6,67
157,5	0,78	7,33
160	0,59	8,48
$x^0 = 0,2$, $T = 1000$ K		
105	0,96	3,34
107,5	0,89	3,26
110	0,82	3,23
112,5	0,75	3,27
115	0,66	3,41
117,5	0,56	3,63
120	0,44	4,20
122,5	0,27	5,07
125	0,04	6,56
$x^0 = 0,2$, $T = 1500$ K		
122,5	0,99	5,15
125	0,91	5,14
127,5	0,82	5,20
130	0,73	5,36
132,5	0,62	5,64
135	0,49	6,12
137,5	0,33	6,87
140	0,12	8,02
$x^0 = 0,2$, $T = 2000$ K		
140	0,97	6,23
142,5	0,87	6,24
145		6,33
147,5	0,64	6,53
150	0,50	6,87
152,5	0,33	7,41
155	0,13	8,23
$x^0 = 0,3$, $T = 1000$ K		
95	0,95	3,80
97,5	0,88	3,59
100	0,82	3,41
102,5	0,75	3,29
105	0,68	3,21
107,5	0,60	3,19
110	0,52	3,24
112,5	0,42	3,39
115	0,31	3,68
117,5	0,17	4,17

P, kbar	ξ	$\frac{dT}{dP}$, $\frac{K}{kbar}$
$x^0 = 0,3$, $T = 1500$ K		
112,5	0,95	5.50
115	0,86	5,36
117,5	0,78	5,27
120	0,69	5,22
122,5	0,60	5,24
125	0,51	5,33
127,5	0,40	5,3
130	0,27	5,85
132,5	0,12	6,36
$x^0 = 0,3$, $T = 2000$ K		
127,5	0,98	6,78
130	0,89	6,64
132,5	0,79	6,54
135	0,69	6,47
137,5	0,59	6.45
140	0,47	6,49
142,5	0,35	6,62
145	0,20	6,85
147,5	0,04	7,22
$x^0 = 0,5$, $T = 1000$ K		
80	0,94	5.13
82,5	0,83	4,65
85	0,74	4,24
87,5	0,66	3,89
90	0,58	3,60
92,5	0,51	3,36
95	0,44	3,16
97,5	0,36	3,01
100	0,29	2,92
102,5	0,21	2.88
105	0,12	2,91
107,5	0,02	3,02
$x^0 = 0,5$, $T = 1500$ K		
95	0,93	6,75
97,5	0,82	6,37
100	0,71	6,05
102,5	0,61	5,77
105	0,52	5,54
107,5	0,43	5,36
110	0,34	5,23
112,5	0,25	5,14
115	0,15	5,11
117,5	0,05	5,15
$x^0 = 0,5$, $T = 2000$ K		
110	0,88	7,89
112,5	0,76	7,60
115	0,65	7,34
117,5	0,55	7,13
120	0,45	6,95
122,5	0,35	6,80
125	0,25	6,69
127,5	0,14	6,62
130	0,03	6,59

Table 4 (Continued)

P, kbar	ξ	$\frac{dT}{dP}, \frac{K}{kbar}$
$x^0 = 0,7$, $T = 1000$ K		
70	0,83	6,69
72,5	0,67	5,74
75	0,55	4,97
77,5	0,44	4,34
80	0,36	3,84
82,5	0,28	3,43
85	0,21	3,10
87,5	0,14	2,83
90	0,07	2,62
$x^0 = 0,7$, $T = 1500$ K		
82,5	0,85	8,31
85	0,67	7,58
87,5	0,53	6,94
90	0,41	6,39
92,5	0,30	5,93
95	0,20	5,55
97,5	0,10	5,24
100	0,01	4,99
$x^0 = 0,7$, $T = 2000$ K		
95	0,83	9,45
97,5	0,65	8,90
100	0,50	8,39
102,5	0,36	7,95
105	0,24	7,55
107,5	0,13	7,22
110	0,03	6,94
$x^0 = 0,9$, $T = 1000$ K		
60	0,90	10,83
62,5	0,45	8,13
65	0,24	6,06
67,5	0,12	4,61
70	0,02	3,60
$x^0 = 0,9$, $T = 1500$ K		
72,5	0,51	10,24
75	0,24	8,61
77,5	0,07	7,24
$x^0 = 0,9$, $T = 2000$ K		
82,5	0,56	11,42
85	0,25	10,31
87,5	0,05	9,25

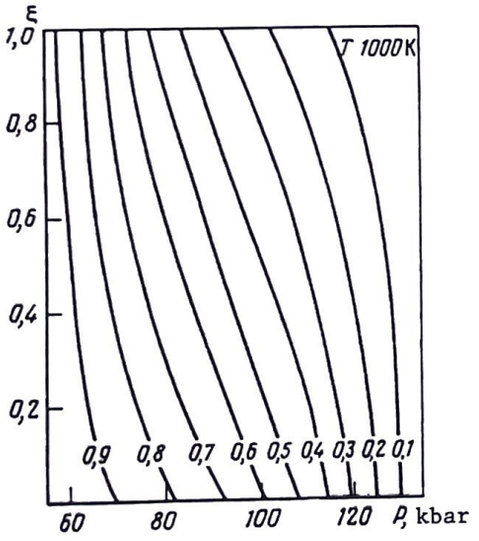

Fig. 3. Equilibrium values of the degree of transformation in the divariant two-phase region for various values of the over-all composition in the olivine-spinel transformation (see Fig. 2). The numbers correspond to the concentrations of the fayalite component.

It was assumed that

$$T\frac{\partial S_{\alpha,\gamma}}{\partial T} \equiv c_{p_{\alpha,\gamma}} = x_{\alpha,\gamma} c^{Fe}_{p_{\alpha,\gamma}} + (1 - x_{\alpha,\gamma})\, c^{Mg}_{p_{\alpha,\gamma}}$$

$$-\frac{\partial S_{\alpha,\gamma}}{\partial P} \equiv \alpha_{\alpha,\gamma} V_{\alpha,\gamma} = x_{\alpha,\gamma} \alpha^{Fe}_{\alpha,\gamma} V^{Fe}_{\alpha,\gamma} + (1 - x_{\alpha,\gamma})\, \alpha^{Mg}_{\alpha,\gamma} V^{Mg}_{\alpha,\gamma}.$$

The data of Table 4 enable us to examine the fine structure of the adiabat in the divariant region. In particular, the pressure dependence of $(dT/dP)_A$

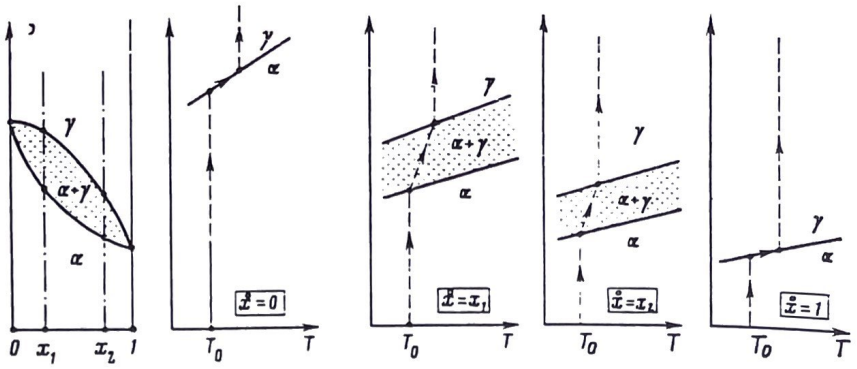

Fig. 4. Simple phase diagram for a binary system with unrestricted miscibility and the corresponding types of adiabat in $P-T$ coordinates. The adiabat family has been parameterized by means of the bulk mixture composition.

is not monotonal* in the region of intermediate compositions. In the magnesium-rich region, the largest temperature increase occurs near the spinel stability region, while for iron-rich solutions it occurs near the olivine boundary of the divariant zone. If we take the mean value of ~5 K/kbar for $(dT/dP)_A$, we find that the temperature step in the divariant heterophase region for $\mathring{x} = 0.1$ is $\delta T \sim 50$-75 K. The phase diagram (Fig. 2) enables us to calculate the correction for the nonisothermal behavior to the pressure difference in the transformation zone, which is $\delta_T P \sim 1.8$-2.7 kbar or $\delta_T l_0 \sim 5.0$-7.5 km. The width of the divariant region at 1000-2000 K is then 33-50 km.

We thus conclude that the adiabatic gradient in the divariant region constructed on the basis of phase equilibrium considerably exceeds the mean value of $(dT/dP)_A$ for each of the participating phases (< 1 K/kbar) because there is not only the ordinary heat production on adiabatic compression but also a phase transition and the corresponding component redistribution between phases. As the mantle is composed of multicomponent minerals, between which there may be many transformations, we conclude that one cannot use a chemically inert mixture in the simulation to calculate the adiabatic gradient for regions homogeneous in phase composition.

Let us consider the family of adiabats in $P-T$ coordinates parameterized by means of $\mathring{x}$, which specifies the overall composition, and trace the deformation of these curves as $\mathring{x}$ varies. Figure 4 shows a series of adiabats corresponding to a simple phase diagram of cigar type. For compositions corresponding to the pure phases, the adiabat has a kink on the monovariant equilibrium line [4, 9]. A similar argument can be applied for more general phase diagrams. We assume that there is a third phase in the composition range enriched in one component, which corresponds to the actual Mg_2SiO_4-Fe_2SiO_4 system in the relevant pressure and temperature range. Figure 5 shows that the adiabat structure can be more complicated in this case. In particular, an additional curve appears in the $P-T$ plane corresponding to nondegenerate univariant equilibrium between the three phases** α, β, and γ. A characteristic feature of these adiabats is the presence of extended zones with anomalous temperature gradients (the gradients exceed that in a chemically inert medium by a substantial factor), which are separated by temperature "steps," where the gradient may exceed the mean by two orders of magnitude. A similar structure will occur in the seismic profile: the extended divariant regions should be represented by gradient zones, while the monovariant transformations will generate adjacent sharper features. Such structures have been detected in seismic experiments [19], so one hopes that improved resolving power in seismic sounding methods should make it possible to extract information on the overall compositions of abyssal rocks from the shape of the seismic profile.

---

*We have restricted ourselves to calculating $(dT/dP)_A$ at specific points. To integrate (22) would be premature on account of the residual uncertainty in the initial parameters.

**The univariant α-γ curves for the end-members of the solid solution series are degenerate, since the compositions of the two phases coincide.

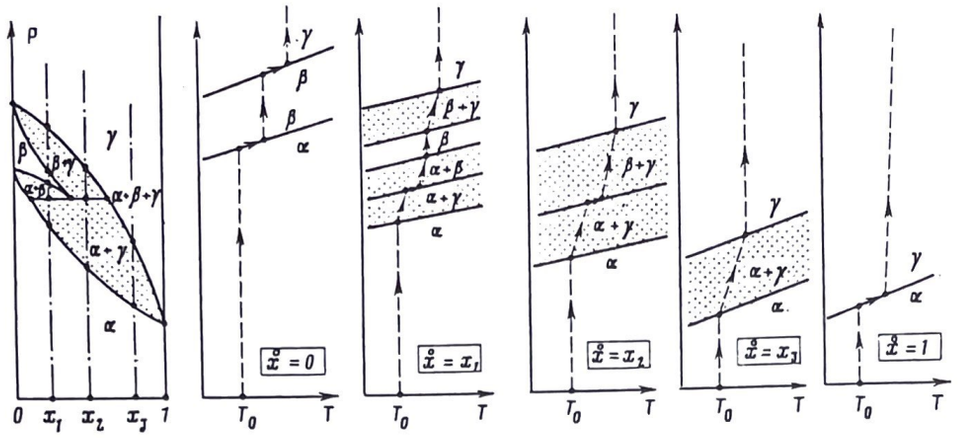

Fig. 5. Phase diagram for a binary system containing three phases (unrestricted miscibility) and the corresponding types of adiabat in $P-T$ coordinates. The adiabatic family has been parameterized by means of the bulk composition.

CONCLUSIONS

The study concerns simulating the structure of a divariant heterophase region in a convecting mantle and the construction of adiabats when heat sources are present due to chemical and phase transformations. This model has been chosen because we need to construct an adequate model for the geochemical structure of the transition zone. There are considerable difficulties in interpreting the anomalous behavior of the seismic velocities in this part of the mantle [19]. Seismology indicates that there is considerable fuzziness in the gradient regions, explaining which is fairly complicated in terms of univariant transformations. It is therefore necessary to have a thermodynamic simulation of the divariant zones, by which is meant minerals of solid-solution type making up the mantle rocks. The resulting information can be used to calculate model distributions for the density and elastic moduli (seismic-wave velocities), which allow direct comparison with seismic data.

The general theoretical section deals with the thermodynamic structure of the adiabat (isentrope) for divariant multiphase regions. Equations have been derived in differential form for the pressure dependence of the phase compositions, which represent a generalization of the van der Waals equations for binary systems. These equations give an expression for $(dT/dP)_A$ along the adiabat; a detailed discussion has been conducted for a binary system with ideal mixing.

A study has been made of the simple two-component forsterite-fayalite system by constructing a thermodynamically correct phase diagram, which has shown that the α-γ phase transition in the olivine solid solution leads to the formation of a two-phase zone of considerable width, which has substantial heterogeneity. The main result is that the adiabatic gradient has an anomalously high value in the divariant region, which is due to there being additional energy sources of chemical origin.

We thus note the following features. Thermal mantle models are usually constructed without allowance for the complicated composition and possible solid-state transformations, which leads to certain paradoxes. For example, the adiabatic gradients in the stability regions of individual mantle phases and of the corresponding mechanical mixture are on average 0.6-0.8 K/kbar. If the temperature at the boundary between the upper mantle and the transition zone is 1400-1600°C, we get $T \sim 2500$°C for a core-mantle boundary, which is clearly insufficient to melt the outer core. The proposed solutions amount to introducing impermeable thermal boundary layers, with considerable temperature differences [20]. These hypothetical constructions have no direct confirmation. On the other hand, chemical and phase transformations in mantle minerals are indisputable and confirmed by experiment. Taking into account the heat production at the univariant phase boundaries during convection, one finds that there are temperature steps in the transition zone [4, 9], which considerably increase the effective adiabatic gradient. The divariant equilibrium associations occurring in the mantle may give an adiabatic gradient five times the mean value for regions where an analogous mechanical phase mixture exists, which increases the temperature at the lower mantle boundary by hundreds of degrees.

Long-range extrapolations are of course liable to error. Nevertheless, this analysis indicates major energy effects accompanying convection in multicomponent multiphase media, and these deserve detailed attention. When these effects are incorporated, existing approaches to simulating the Earth's thermal history may need to be modified.

REFERENCES

1. Zharkov, V.N. and V. P. Trubitsyn, 1980. Fizika planetnykh nedr [Physics of Planetary Interiors], Nauka, Moscow.
2. Myasnikov, V.P. and V. Ye. Fadeyev, 1980. Modeli evolyutsii Zemli i planet zemnoy gruppy [Models for the Evolution of the Earth and the Terrestrial-Group Planets], VINITI, Moscow.
3. Truskinovskiy, L.M., 1984. Matematicheskiye modeli tverdofazovykh prevrashcheniy v perekhodnoy zone mantii [Models of Solid-State Reactions in the Mantle Transition Zone: Ph. D. Thesis], IFZ AN SSSR, Moscow.
4. Truskinovskiy, L.M., O. L. Kuskov and N. I. Khitarov, 1983. Geokhimiya, No. 9, p. 1222.
5. Saxena, S., 1975. Thermodynamics of Rock-Forming Mineral Solid Solutions [Russian translation], Mir, Moscow.
6. Kuskov, O.L., R. F. Galimzyanov, V. A. Kalinin, et al., 1982. Geokhimiya, No. 7, p. 984.
7. Shubert, G., D. A. Yuen and D. L. Turcotte, 1975. Geophys. J. Roy. Abstr. Soc., v. 42, No. 2, p. 705.
8. Kadik, A.A. and M. Ya. Frenkel', 1982. Dekompressiya porod kory i verkhney mantii kak mekhanizm obrazovaniya magm [Crustal and Upper-Mantle Rock Decompression as a Magma Formation Mechanism], Nauka, Moscow.
9. Truskinovskiy, L.M., O. L. Kuskov and N. I. Khitarov, 1984. Dokl. AN SSSR, v. 274, No. 5, p. 1064.
10. Gibbs, J.W., 1950. Thermodynamic Papers [Russian translation], Tekhteorizdat, Moscow and Leningrad.
11. Ostapenko, G.T., 1971. Zh. Fiz. Khimii, v. 45, No. 6, p. 1386.
12. Kurosh, A.G., 1967. Kurs vysshey algebry [Textbook of Higher Algebra], Nauka, Moscow.
13. Van der Waals, J. and F. Constamm, 1936. Textbook of Thermostatics [Russian translation], v. 2, Izd. ONTI, Moscow.
14. Prigogine, I. and R. Defay, 1966. Chemical Thermodynamics [Russian translation], Nauka, Novosibirsk.
15. Kuskov, O.L., R. F. Galimzyanov, L. M. Truskinovskiy, et al., 1983. Geokhimiya, No. 6, p. 849.
16. Kuskov, O.L., 1984. Geokhimiya, No. 8, p. 1719.
17. Ringwood, A.E., 1981. Composition and Petrology of the Earth's Mantle [Russian translation], Nedra, Moscow.
18. Jeanlos, R. and A. Thompson, 1983. Rev. Geophys. Space Phys., v. 21, No. 1, p. 51.
19. Vinnik, L.P., 1984. Dokl. AN SSSR, v. 274, No. 2, p. 296.
20. Jeanlos, R. and F. M. Richter, 1979. J. Geophys. Res., v. 84, p. 5497.